ELSEVIER

Polymer 42 (2001) 7893–7901

polymer

www.elsevier.nl/locate/polymer

Mechanically stable copolyimide for low level stress buffer

Hyunsoo Chung, Jongwhae Lee, Jaewook Hwang, Haksoo Han*

Department of Chemical Engineering, Yonsei University, 134 Shinchon-dong, Seodaemun-gu, Seoul 120-749, South Korea

Received 24 August 2000; received in revised form 15 January 2001; accepted 8 February 2001

Abstract

Copolyimide thin films, which has the low level stress and stress relaxation induced by water sorption, were characterized for potential application as encapsulant, stress-relief buffer, and interlayer dielectrics. The polyimides studied are poly(*p*-phenylene pyromellitimide) (PMDA-PDA), poly(*p*-phenylene 4,4′-hexafluoroisopropylidene diphthalimide) (6FDA-PDA) and their random copolyimides with various composition. These copolyimide films exhibited good combinations of physical and mechanical properties with low thermal expansion coefficient (TEC) and residual stress behavior by appropriately selecting the ratios of the acid dianhydride component. For these copolyimides, residual stress increased in the range of −5 to 50 MPa, whereas stress relaxation induced by water uptake decreased in the range of 20.5–4.5 MPa at 30°C, 100% relative humidity with increasing 2,2′-bis(3,4-dicarboxyphenyl) hexafluoropropane dianhydride (6FDA) composition, respectively. The degree of in-plane chain orientation was directly correlated to the residual stress and stress relaxation coefficient (*S*) in the film, which is an in-plane characteristic. However, the stress relaxation caused by the water uptake was significantly influenced by packing order induced by chain mobility, which might occur during thermal imidization. Overall, the candidate for the low level stress buffer application from the PMDA/6FDA-PDA copolyimide was both the 90/10 (= PMDA/6FDA in molar ratio) and 70/30 copolyimides. © 2001 Elsevier Science Ltd. All rights reserved.

Keywords: Copolyimide; Residual stress; Stress relaxation

1. Introduction

Future multichip packing technologies are expected to benefit from the use of polymers as interlayer dielectrics, passivation layers and alpha particle barriers because of their high thermal stability, relatively low dielectric constant, high chemical resistance and easy processability [1–4]. Despite their many advantages, the tendency of polyimide films to absorb moisture can pose serious reliability problems, such as corrosion, internal shorts, delamination, loss in dimensional stability, and reduction in mechanical performance. Consequently, many studies have been conducted on the transport and diffusion of moisture in polyimide films [5–8]. Also, the good mechanical properties are essential in multilevel packaging applications due to residual thermal stresses caused by differences in thermal expansion coefficient (TEC) between dissimilar materials used in the multilayer structure [9–13]. However, these requirements of polymer properties for more advanced microelectronic applications are quite severe such that they cannot be usually met by a single component polymer [14,15] Moreover, more functionality is demanded of polymer dielectrics without compromising the existing properties.

Research conducted over the past decade has understood the importance of considering the polymer film morphology contributions to the residual stress and its moisture-induced stress relaxation behavior of polymer films [5,6,16–19]. Poly(*p*-phenylene pyromellitimide (PMDA-PDA) film is well known as a fully rod-like polymer with low residual stress and low TEC, which are highly required in the fabrication of microelectronic devices [20]. This approach is very limiting with respect to the number of possible rigid rod-like structures obtainable and synthetic flexibility. In addition, fully rod-like PMDA-PDA exhibits a high modulus, but is too brittle and fragile for application as well as inherently poor adhesion properties. One approach to obtain the combination of desired properties is copolymerizing a rod-like polyimide system with a flexible and hydrophobic component. This could provide enhanced adhesion, increased toughness and low level water sorption without sacrificing low TEC, high modulus of elasticity, and thermal stability of polymer film. Especially, polyimide with bulky di(trifluoromethyl) (CF_3) groups has high transparency, low dielectric constant, high gas permeability and water resistance as merits [21–23].

---

* Corresponding author. Tel.: +82-2-2123-2764; fax: +82-2-312-6401.
E-mail address: hshan@yonsei.ac.kr (H. Han).

0032-3861/01/$ - see front matter © 2001 Elsevier Science Ltd. All rights reserved.
PII: S0032-3861(01)00214-2

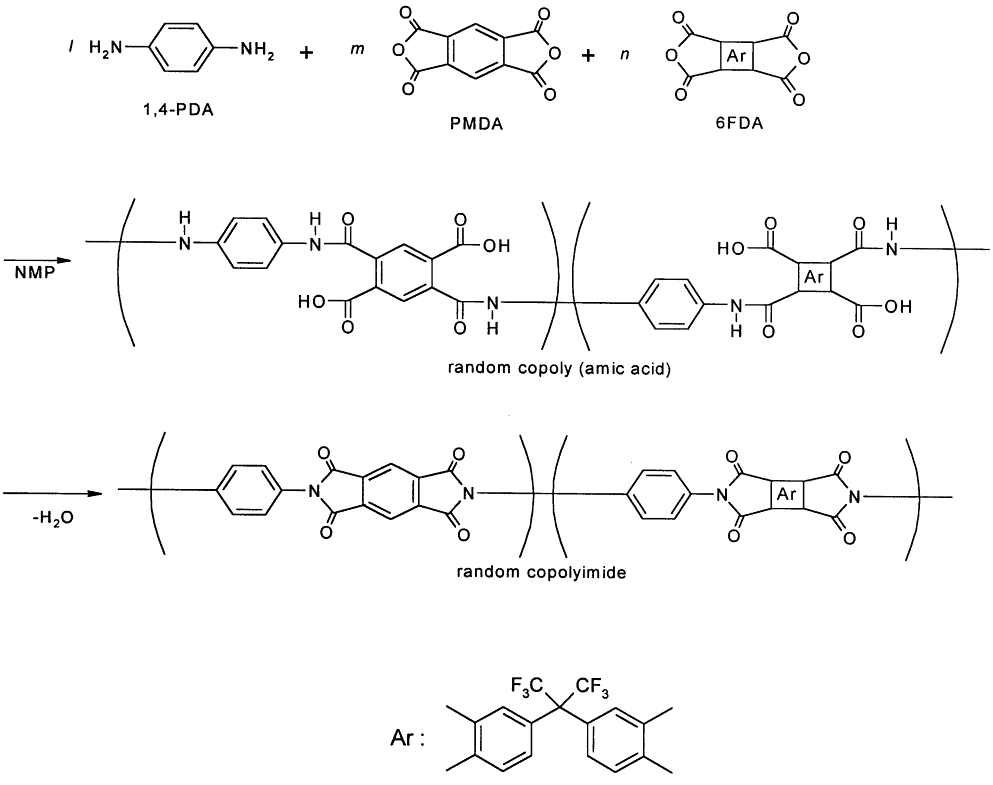

Fig. 1. PMDA/6FDA-PDA copolyimide films by thermal imidization at 400°C.

Poly(amic acid)s (PAAs) of PMDA/6FDA-PDA polyimides with various 2,2′-bis(3,4-dicarboxyphenyl) hexafluoropropane dianhydride (6FDA) composition were synthesized as a route to low stress polyimide as well as structural modification and their effects on the morphology and mechanical properties. The 6FDA units contributed to a lower glass transition temperature (T_g) and water uptake, and the PDA contributed to a lower TEC. To achieve the advantageous property characteristics including low stress and moisture-induced stress relaxation, PMDA/6FDA-PDA were used to investigate their morphological structure and properties. Also, it should be possible that the high brittleness of rod-like PMDA-PDA polyimide is successfully healed with only a minor effect on the high modulus by incorporating 6FDA into the polymer backbone.

The residual stress in the copolyimides with different 6FDA composition were measured using a thin film stress analyzer (TFSA) over the processing temperature from 25–400°C. And then, the moisture-induced stress relaxation of fully cured copolyimide was measured at 30°C in 100% relative humidity (RH) in TFSA and analyzed by the Fickian process. These stress behaviors were interpreted with the consideration of the morphological structure, chain mobility, and thermal expansion parameter. For the characteristic properties of polyimide thin films, morphological structures were examined using wide-angle X-ray diffraction (WAXD) and prism coupler, for the chain mobility, using dynamic mechanical thermal analyzer (DMTA) and thermal expansivity by thermal mechanical analyzer (TMA).

2. Experimental

2.1. Material and sample preparation

PAAs were synthesized in dry 1-methyl-2-pyrrolidinone (NMP) at a concentration of 15% solids (w/w) by adding a stoichiometric amount of the combination of dianhydrides in a powder form to a mechanically stirred solution of the *p*-phenylene diamine (PDA) under nitrogen atmosphere at room temperature as shown in Fig. 1. Pyromellitic dianhydride (PMDA) and *p*-phenylene diamine were vacuum sublimed (Aldrich Co.). 2,2′-bis(3,4-dicarboxyphenyl) hexafluoropropane dianhydride (6FDA) was obtained from TCI Co., Ltd., and sublimed prior to use. NMP was used as received from Aldrich Co.

PAAs were synthesized using an equimolar amount of dianhydride or combination of dianhydride with diamine. For the preparation of copolyimides, the ratio of anhydrides (PMDA/6FDA) employed were 90/10, 70/30, 50/50, 30/70, respectively. All precursor solutions were spin coated on silicon wafers and soft baked at 80°C for 1 h. In addition, precursor films were prepared on polished wafers that were coated with an adhesion primer, 0.1 vol% r-aminopropyltriethoxy silane solution in 90 vol% ethanol/10 vol% water, and then used for dynamic stress measurements to prevent the partial detachment of the film. The stress relaxation behaviors of polyimide films were measured after conventional thermal imidization from 25–400°C. The ramping rate was 2.0°C/min, and the cooling rate was 1.0°C/min. In addition, the thicknesses of polyimide films were controlled range of 9–11 μm to exclude the thickness effect. The one-side polished Si(100) wafer as substrate used in this study was 76.2 mm diameter.

2.2. Measurement

The residual stresses of films were measured during thermal imidization with cure process and subsequent cooling, using a double He–Ne laser beam based TFSA [16–20,24–26]. To determine the residual stress from the measured radii of curvature, a well-known Eq. (1) was employed [27]. The residual stress was calculated from the measured radii of curvature using the following equation:

$$\sigma = \frac{E_s}{6(1-\nu_s)} \frac{t_s^2}{t_f} \left(\frac{1}{R_2} - \frac{1}{R_1} \right), \quad (1)$$

where σ is the residual stress in the polyimide film. The subscripts, f and s denote the polyimide film and the substrate. E, ν, and t are Young's modulus, Poisson's ratio, and the thickness of the substrate, respectively. R_1 and R_2 are the wafer curvatures measured before and after the film deposition. For Si(100) wafer, $E_s/(1-\nu_s)$ is 180 500 MPa [28]. Before use, the initial curvature and the thickness of wafers were measured by using the TFSA and the thickness gauge (SM1201, Teclock Co., Japan).

Stress relaxation due to water diffusion can be determined by the measurement of the stress difference as a function of time. Stress relaxation is generally due to creep as well as moisture uptake in polymer film. The film stress relaxation at a highly supercooled state is predominated by the moisture uptake in humid environments due to the restricted chain mobility [24–26]. For high temperature polyimides having relatively high glass transition temperature, creep-induced stress relaxation at room temperature is small to overall stress relaxation. Thus, the stress relaxation is mainly caused by the moisture so that the rate of stress reduction may reflect that of water absorbed by the film. For films in which the moisture uptake obeys Fick's law, the stress relaxation rate can be estimated by best fitting the moisture-induced stress relaxation versus time curves. Thus, the stress relaxation of polyimide thin film can be expressed quantitatively from a macroscopic viewpoint by Fick's laws of diffusion [29–31]. If $\sigma_w(t)$ is the stress induced by water diffusion at time t and $\Delta\sigma$ is the difference between the stresses at $t=0$ and $t=\infty$, then Eq. (2) gives the time dependence of stress in terms of the stress relaxation coefficient (S), and thickness (L) of thin film.

$$\frac{\sigma_0 - \sigma_w(t)}{\Delta\sigma} = 1 - \frac{8}{\pi^2} \sum_{n=1}^{\infty} \frac{1}{(2n-1)^2} \times \exp\left[-\frac{\pi^2 (2n-1)^2}{4L^2} St \right]. \quad (2)$$

The experimental data was plotted with stress relaxation ratio $(\sigma_0 - \sigma_w(t))/\Delta\sigma$ as a function of $t^{1/2}L^{-1}$. Using Eq. (2), various values of S were assumed, and error between experiment and relaxation was minimized to produce the fitted apparent stress relaxation coefficient, S.

For the wide angle X-ray diffraction (WAXD) measurements and other characteristic properties, these fully cured films were removed from the substrate after soaking in distilled water for 24 h. They were washed with distilled water several times and dried. WAXD measurements were conducted in the $\theta/2\theta$ method over 3.5–60° using a Rigaku diffractometer (Model D/Max-200B) with CuKα ($\lambda = 1.54$ Å) radiation source. Step and count data were taken at 0.02° intervals a scan speed of 0.4°/min. The measured WAXD patterns were corrected to the background run and then normalized for the film samples by matching the integrated intensity with the range of 58–60° (2θ) [32,33]. For WAXD measurement, transmission runs in which the diffraction vector is in the film plane can provide structural information in the film plane, whereas reflection runs in which the diffraction vector is in the direction normal to the film plane can give structural information in the direction of film thickness. For birefringence of polyimides films, prism coupling patterns were measured using a Metricon prism coupler (Model 2010). The refractive index in the film plane, n_{xy} was measured in the transverse electric (TE) mode, n_z was measured in the transverse magnetic (TM) mode by choosing the appropriated polarization of the incident laser light as described elsewhere [9,20,34–37]. All measurements were performed using a cubic zirconia prism of $n_{TE} = n_{TM} = 2.1677$ at a wavelength of 632.8 nm. The birefringence ($\Delta = n_{xy} - n_z$) is a measure of the molecular orientation in the in-plane of the polyimide thin film.

For the other characteristic property, DMTA (Polymer Lab. MKIII) was used. The employed heating rate and frequency was 5.0°C/min and 1 Hz, respectively. The thermal expansion properties were measured by a thermomechanical analyzer (Du Pont Model 943). The measurements were carried out under nitrogen at a heating rate of 10°C/min.

3. Results and discussion

3.1. Residual stress measurements

The residual stress behaviors measured on Si(100) substrate were shown in Fig. 2, and the analyzed results

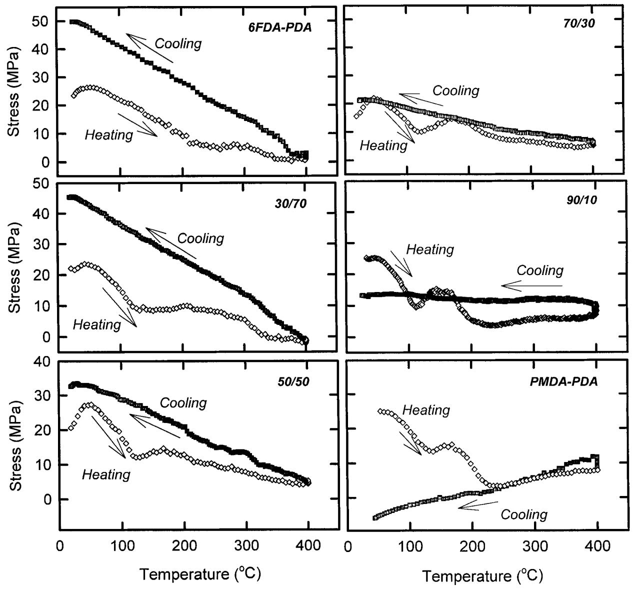

Fig. 2. Residual stress behavior of copolyimide film by thermal imidization at 400°C.

are summarized in Table 1. For the precursor films, the stress was 22–27 MPa, depending on the degree of drying as well as the concentration of 6FDA, 27 MPa for the PMDA-PDA PAA film and ca. 22 MPa for the 6FDA-PDA PAA. The stress difference between these polyimide precursor films is only 5 MPa.

However, the stress behavior of the copolyimide precursor film is strongly dependent on the composition of dianhydrides during thermal curing. For rod-like PMDA-PDA, the residual stress and slope of cooling curve after fully cured at 400°C was −5 and 50 MPa for 6FDA-PDA. As the concentration of 6FDA increased, the residual stress drastically increased to 10–50 MPa for the PMDA/6FDA-PDA copolyimide. The high stress component, 6FDA-PDA significantly influenced the stress in the copolyimide films. On cooling at 400°C, for 6FDA-PDA polyimide with a relatively low T_g, the stress started to increase rapidly at ca. 375°C, whereas for PMDA/6FDA-PDA copolyimide with a high $T_g > 400°C$ increased gradually from 400°C. Even if the small proportion of 6FDA having a flexible linkage is added into the chain structure, the copolyimide structure is disturbed, and a large development of stress occurred. This means that the incorporation of larger bulky fragment into the copolyimide backbone influence the increase in TEC and easier chain mobility.

In particular, for the PMDA-PDA, the residual stress decreased with the cooling temperature in compression mode and varied to −5 MPa at 25°C. This means the curvature of film/substrate warps to the film side and then flips inversely to the substrate side when thermally cycled over 25-400°C. This phenomenon may severely deteriorate the interfacial stability in the package, sometimes leading to the interfacial failure. Therefore, for the substrates coated with polyimide, the level of residual stress should be kept as low as possible in a single mode. This shortcoming in PMDA-PDA may be resolved at once by the incorporation of 6FDA. The PMDA/6FDA-PDA (90/10) significantly improves the toughness of a given brittle PMDA-PDA without sacrificing low residual stress kept in a single mode.

3.2. Stress relaxation measurements

The stress relaxation of PMDA/6FDA-PDA copolyimide films was also studied in ambient air at 30°C, 100% RH at room temperature. In general, the stress of a polymer film on a substrate in air ambient relaxes due to moisture uptake. The stress relaxation results of the copolyimide films are illustrated in Fig. 3. When a copolyimide film on Si substrates was exposed to ambient air with 100% RH, the stress rapidly relaxed with time at the initial stage, thereafter gradually decreased, and finally leveled off. The stress difference between the initial and relaxed states reflects a degree of moisture uptake. The stress relaxation plots show that the PMDA-PDA polyimide relaxed more in comparison with the 6FDA-PDA polyimide. The copolyimide films showed water uptake behavior intermediate between those of the component. The stress relaxation $\Delta\sigma$ was 20.5 MPa for the PMDA-PDA, 17.1 MPa for the 10/90 (= PMDA/6FDA in molar ratio) copolyimide, 11.7 MPa for the 30/70 copolyimide, 9.5 MPa for the 50/50 copolyimide, 7.0 MPa for the 70/30 copolyimide, and 4.5 MPa for the 6FDA-PDA. Therefore, we suspect that the PMDA-PDA films absorb more water in comparison with the 6FDA-PDA because the magnitude of $\Delta\sigma$ in the relaxation may

Table 1
Residual stresses of PMDA/6FDA-PDA polyimides at 30°C after full cure at 400°C for 1 h

Molar ratio PMDA/6FDA	Residual stress after full cure at 25°C (MPa)	Slope in cooling curve (MPa/°C)	Thickness (μm)
0/100	50	0.1287	10.3
30/70	47	0.1199	11.3
50/50	33	0.0781	11.0
70/30	21	0.0423	11.2
90/10	15	0.0012	10.9
100/0	−5	−0.0515	10.7

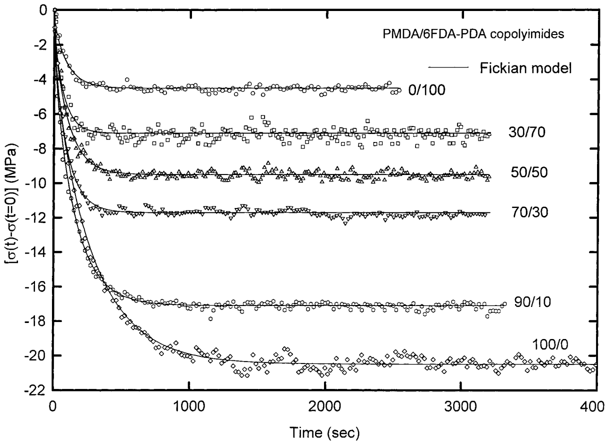

Fig. 3. Moisture-induced residual stress relaxations of the PMDA/6FDA-PDA copolyimide films on Si measured at 30°C and 100% RH as a function of time.

reflect the amount of water absorbed by the film. The initial slope in the $\Delta\sigma$ versus time plot indicates the stress relaxation coefficient induced by moisture diffusion. The steeper slope results from the faster diffusion coefficient in the films. The stress relaxation rate, S was 16.30×10^{-10} cm^2/s for the PMDA-PDA film and 67.38×10^{-10} cm^2/s for the 6FDA-PDA polyimide as shown in Table 2.

These stress relaxation behaviors may be attributed to the difference in their chemical structures or their morphologies. By comparing the chemical structures of PMDA-PDA and 6FDA-PDA, one can attribute the slower stress relaxation induced by water diffusion in the films of 6FDA-PDA to the presence of the $-C(CF_3)_2$-hexafluoroisopropylidene linkage. This linkage can be treated as a diffusion unfavorable site since it is hydrophobic [37–39]. However, stress relaxation rate of 6FDA-PDA is much more rapid than that in PMDA-PDA films. From this standpoint, the significant difference between their stress relaxation rates can be attributed to the morphological difference in their crystallinity or packing order. However, the extent of stress relaxation of rod-like PMDA-PDA having higher crystallinity is significantly higher than that of amorphous 6FDA-PDA. This suggests that PMDA-PDA has morphological defect for the water uptake.

Table 2
Residual stress relaxation behavior of PMDA/6FDA-PDA polyimides at 30°C after full cure at 400°C for 1 h

Molar ratio PMDA/6FDA	Stress relaxation coefficient, S ($\times 10^{-10}$ cm^2/s)	Stress relaxation, ΔS
0/100	16.30	20.5
30/70	25.20	17.1
50/50	40.40	11.7
70/30	42.85	9.5
90/10	54.56	7.0
100/0	67.38	4.5

3.3. Morphological structure

The morphological structures of the homopolyimides and the copolyimides from four composition system can be obtained from WAXD patterns of the polyimides shown in Fig. 4.

For PMDA-PDA, the transmission pattern apparently shows multiple diffraction peaks from the high chain ordering along the chain axis, but exhibits only on amorphous halo peak in the reflection pattern. These indicate that PMDA-PDA chains are mainly oriented in the film plane and highly ordered due to the rod-like chain nature, but irregularly packed together. The lack of regular intermolecular packing might be the result of the limited chain mobility due to its high glass transition temperature.

The transmission patterns show that the (00l) peaks were affected by the 6FDA-PDA composition. The (00l) peak became weak and broad as the concentration of the 6FDA component increased. The (00l) peaks were significantly broadened in the film imidized from the copolyimide precursor with only 30 mol% 6FDA-PDA, and almost disappeared particularly for the film from the copolyimide from the precursor with 50 mol% 6FDA-PDA. The multiple (00l) peaks have appeared only in the transmission geometry in >50 mol% PMDA-PDA ratio, indicating that the polyimide molecules ordered highly along the chain axis are preferentially aligned in the film plane. For this reason, the residual stress of both the 90/10 and 70/30 copolyimide revealed relatively low level because higher in-plane orientation in the film causes low in-plane TEC, causing low stress in the tension mode. In fact, the PMDA-PDA has only a rod-like conformation per repeat unit with a limited rotational freedom, resulting in the inherent high chain order along the chain axis. Thus, the weakening of the higher ordered (00l) peaks for the copolyimide films containing above 50 mol% 6FDA molar ratio might result from the disturbance of the molecular in-plane orientation caused by the bulky di(trifluoromethyl) groups.

The reflection pattern was also influenced by the 6FDA fragment. 6FDA-PDA polyimide revealed structureless WAXD patterns. 6FDA-PDA showed three broad peaks in the reflection as well as the transmission pattern. The first diffraction peak at 15.34° can be assigned as the first order amorphous halo, consequently giving the mean intermolecular distances of 5.8 Å. These might result from very poor chain ordering caused by the bulky di(trifluoromethyl) group. The PMDA-PDA showed an amorphous halo at 21°. However, the amorphous halo is relatively much sharper in shape and in intensity for the PMDA-PDA than the 6FDA-PDA. Also, this amorphous halo shifted left and the intensity of the halos drastically decreased as the content of 6FDA-PDA increased in the copolyimide. This means that the population of the ordered phase is higher in the PMDA-PDA than in the 6FDA-PDA.

Generally, water diffusion probably occurs in the amorphous region with looser molecular packing. 6FDA-PDA

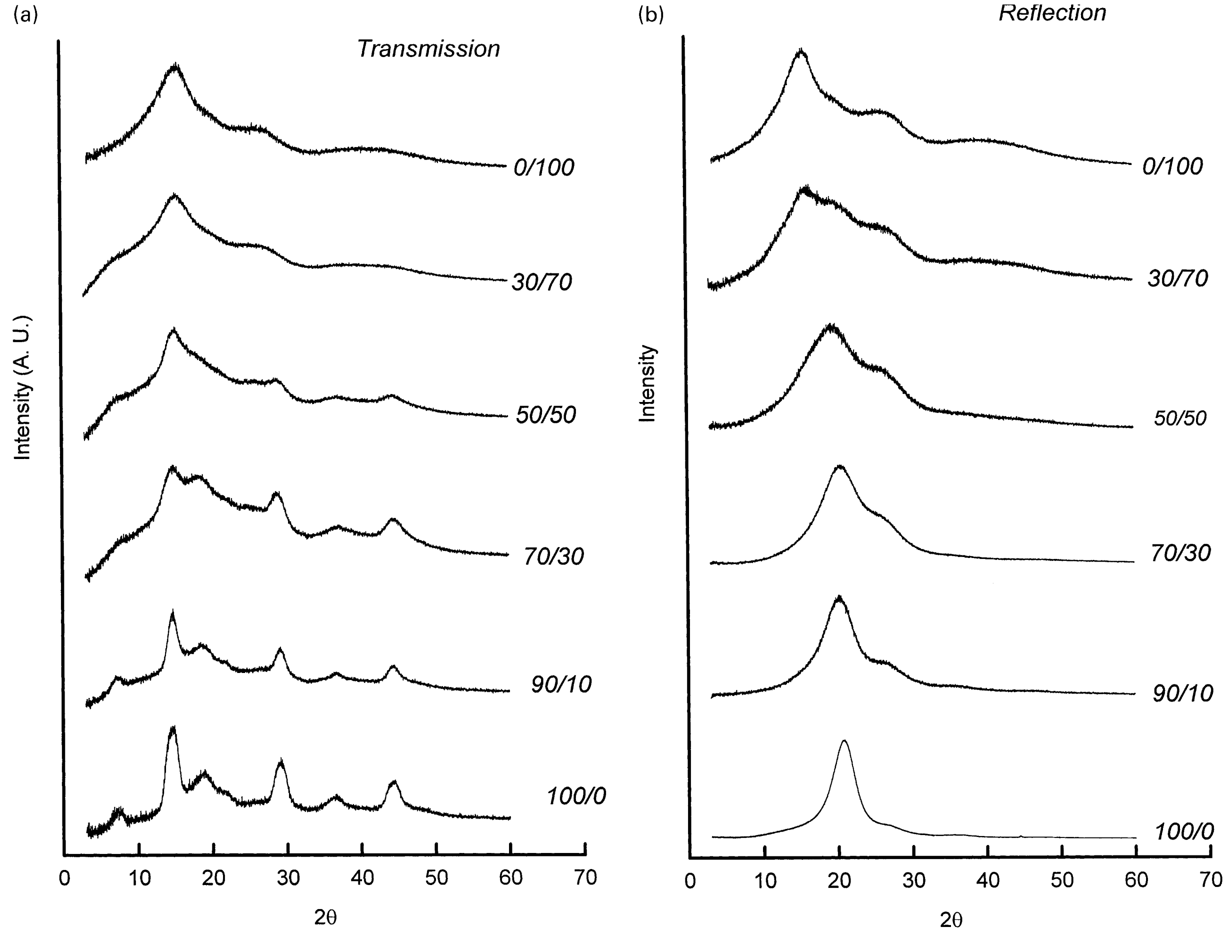

Fig. 4. WAXD patterns of PMDA/6FDA-PDA copolyimide films.

indeed leads to lower crystallinity and, simultaneously, to looser molecular packing in the amorphous region in WAXD. This suggests that morphological structures, such as lower population of ordered phase and crystallinity in 6FDA-PDA polyimide leads to a higher stress relaxation rate (*S*) despite having hydrophobic hexafluoroisopropylidene linkage. This result indicates that the major factor in determining the magnitude of the stress relaxation rate induced by water diffusion in films should be the morphological factor rather than water affinity.

However, stress relaxation variations in the copolyimides do not follow this prediction. PMDA-PDA exhibited the highest stress relaxation in spite of small mean intermolecular distance and higher crystallinity, compared to the other copolyimides. These may be attributed to high levels of morphological defects, e.g. relatively large-scaled free volume and voids possibly formed by the insufficient chain mobility due to rod-like chain characteristics during the thermal imidization. As a result of the high T_g over the final curing temperature of curing process, there will be very limited mobility and less degree of chain relaxation to permit any chain organization, which may result in poor packing order and the morphological defects for water uptake [5,6,17,25]. Compared to the reflection patterns of PMDA-PDA, similar reflection patterns were observed for the other copolyimides; however, the additional shoulder diffraction peaks at 20–30° were found as the 6FDA composition increases. This shoulder diffraction peak in the reflection pattern may be related to the intermolecular packing order. From the peaks of this range, it is speculated that the packing order in the ordered phase increased with increasing 6FDA units. This indicates that chain mobility during thermal process is also important to the degree of stress relaxation due to water uptake.

The molecular orientation in the polyimide was further studied by film refractive indices and birefringence measurement. The results are summarized in Table 3. The in-plane refractive index (n_{xy}) and the out-of-plane refractive index (n_z) at a wavelength of 632.8 nm varied in the ranges 1.7168–1.7474 and 1.6409–1.6595 depending on those of components, respectively. The estimated film birefringence, which is a measure of molecular orientation, increased from 0.0705 to 0.0925 as ratio of 6FDA decreased. This indicates that the high level of in-plane orientation of rod-like polyimide chains gets disturbed with increasing 6FDA. During the thermal imidization, the presence of the bulky hexafluoroisopropylidene groups may increase the tendency such that the polymer molecules are

Table 3
Optical properties in thin films of polyimides

Molar ratio PMDA/6FDA	Refractive index[a]		Birefriengence	Film thickness (μm)
	In-plane (n_{xy})	Out-of-plane (n_z)		
0/100	1.5844	1.5752	0.0092	10.3
30/70	1.6141	1.5879	0.0262	11.3
50/50	1.6535	1.5875	0.0660	11.0
70/30	1.7012	1.5886	0.1126	11.2
90/10	1.7617	1.5892	0.1725	10.9
100/0	1.8202	1.5902	0.2300	10.7

[a] Measured at 632.8 nm (i.e. 474.08 THz).

randomly oriented in the film, ultimately leading to a decrease in the in-plane orientation of polymer chains. Therefore, the higher thermal mismatch-induced residual stress in the tension mode and faster moisture-induced stress relaxation in the compression mode in the copolyimide result mainly from the disturbance of molecular in-plane orientation (lower birefringence) in film, as presented in Table 3.

3.4. Thermal properties

In addition to the molecular order and orientation, the chain mobility should be considered as a key factor in influencing the stress behavior. The chain mobility is directly related to the T_g, which is a measure of chain flexibility. In other words, the temperature and magnitude of the mechanical relaxation are critically dependent upon the chain rigidity, ordered structure, and cooperativeness of the segmental motion. Higher chain flexibility leads to lower T_g, providing higher chain mobility. T_gs of the polyimide were examined as shown in Fig. 5. Here, for each copolyimide, the dynamic mechanical properties (storage modulus and tan δ) were superimposed to compare them with the temperature range 25–500°C. All the copolyimides exhibited a single T_g, which vary between those of the components.

PMDA-PDA did not show glass transition over 50–500°C, indicating that its T_g is higher than 500°C, whereas the 6FDA-PDA showed a relatively sharp glass transition over the range of 350–400°C. The copolyimide films exhibited intermediate glass transition behavior between those of the components. From the tan δ profiles, T_g was estimated to be >460°C for the 70/30 copolyimide, 450°C for the 50/50 copolyimide, 430°C for the 70/30 copolyimide, and 375°C for 6FDA-PDA homopolyimide. In the copolyimide films, T_g decreased as the concentration of 6FDA increased. In particular, the tan δ of 6FDA-ODA showed a sharp glass transition, whereas the other copolyimides relatively exhibited broad transition. It was in good agreement with the absence of (001) peak due to intrinsically amorphous structure in the polyimide thin films based on the morphology.

In comparison to PMDA-PDA, 6FDA-PDA is relatively less rigid. The magnitude of tan δ is sharper and higher than that of copolyimide, indicating that 6FDA-PDA is more mobile. This sharp and high magnitude of tan δ might be due to both lower polyimide chain rigidity and less crystallinity. That is, the accelerated chain mobility induced by lower T_g and crystallinity in 6FDA-PDA during thermal imidization may approve the stress development of fully cured in PMDA/6FDA-PDA. In these results, the tan δ shifts systematically to lower temperature with increasing contents of 6FDA-PDA. This suggests that 6FDA molecules were well dispersed in a matrix of PMDA/6FDA-PDA

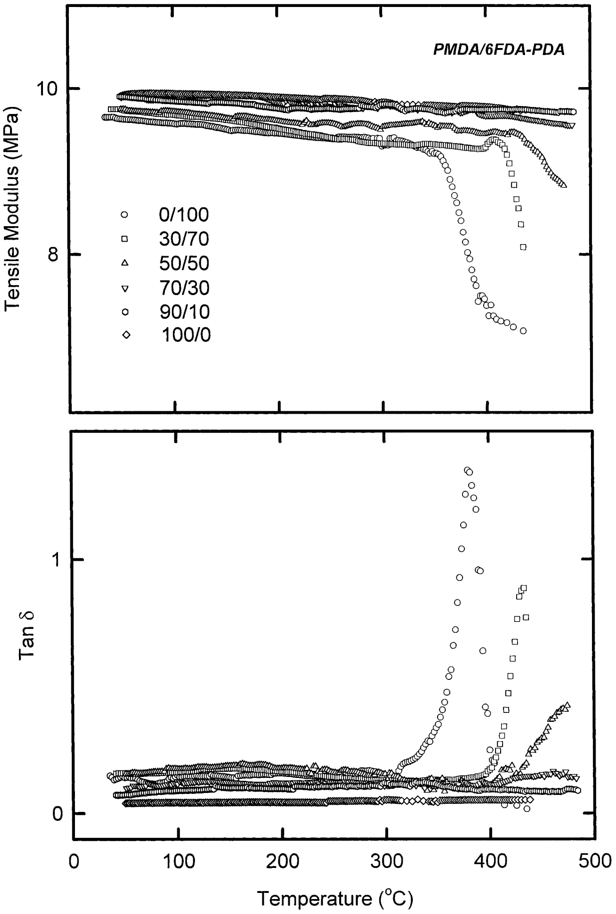

Fig. 5. Temperature dependence of the dynamic tan δ as function of composition. The copolyimide films were thermally imidized at 400°C.

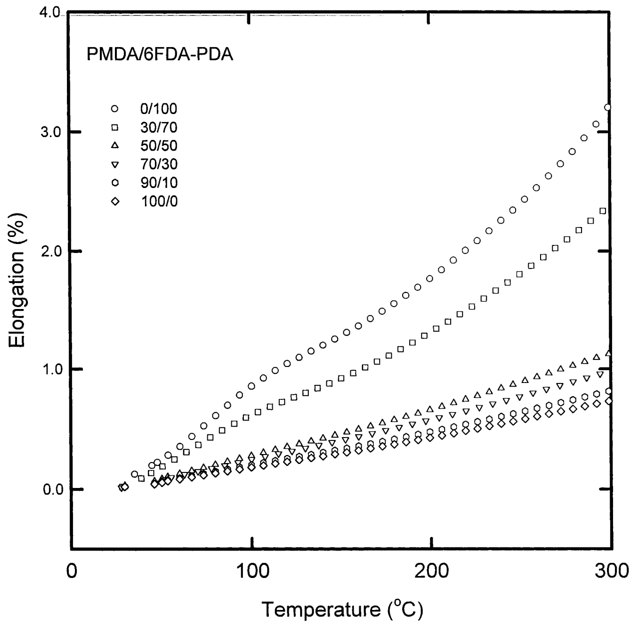

Fig. 6. Thermomechanical analysis for PMDA/6FDA-PDA copolyimide as function of composition.

copolyimide. Additionally, this may be used in explaining why the amount of stress relaxation decreases with the increase in 6FDA incorporation. During thermal imidization, the imidized PMDA-PDA chains are immediately frozen because the T_g is higher than the final imidization temperature (400°C). Under this circumstance, microvoids generated in thermal imidization process may not be healed completely. The limited chain mobility may contribute to the relatively high water uptaking site and then higher stress relaxation. Thus, unfavorably high stress relaxation due to water uptake in rod-like PMDA-PDA having morphological defect due to its high T_g, decrease as the 6FDA-PDA composition having more chain mobility increase during thermal imidization.

The film stress is mainly contributed by the thermal stress component, which is proportional to several factors, such as mismatched TEC (α_s, α_f) and modulus (E). For Si(100), the α_s is 3.0 ppm/°C over 25–400°C. Therefore, the film stress mainly depends on the factors, α_f and E. As shown in Fig. 5, E decreased with increasing concentrations of 6FDA, contributing to the lower film stress. Despite the lowering of stress by the decrease in E, the copolyimide film showed high thermal mismatched stress, indicating that α_f was significantly increased by the 6FDA incorporation. In addition, the relatively low T_g of 6FDA-PDA component may provide relatively high molecular mobility in their copolyimides with PMDA-PDA having undergone thermal curing, consequently allowing a limited level of moisture-induced stress relaxation.

The effect of 6FDA molar ratio on TEC in copolyimide was obtained by TMA from 25 to 300°C under nitrogen at a heating rate of 10°C/min. Fig. 6 shows the effect of compositions of dianhydride on the elongation, temperature behaviors of the copolyimide. As expected from molecular structures and stress behaviors, PMDA-PDA exhibited stiff and hard properties while 6FDA-PDA had a flexible and soft behavior. In Table 4, the elongation was 0.81% for PMDA-PDA, and 3.12% for 6FDA-PDA. Copolyimide films of these components exhibited mechanical properties between those of the components. The slope of the elongation curve became steeper as molar ration of 6FDA increased. This could be attributed to the systematic variation in the film orientations and chain mobility as observed in the X-ray measurement and DMTA results.

4. Conclusion

With 2,2′-bis(3,4-dicarboxyphenyl) hexafluoropropane dianhydride (6FDA), pyromellitic dianhydride (PMDA) and *p*-phenylene diamine (PDA), the homopolyamic acids and copolyamic acids were synthesized and thermally converted to the polyimides in thin films. In this study, the weak elongation and overbrittleness of rod-like PMDA-PDA was successfully healed with only a minor effect on the high modulus and low thermal expansion by incorporating 6FDA into the copolymer backbone having low level of residual stress induced by thermal mismatch between the film and the substrate. In particular, for the (90/10) PMDA/6FDA-PDA copolyimide, the residual stress maintained low level with temperature in tension mode. Thus, for this interfacial stability, addition of <10 mol% 6FDA was proposed to deliver a minimized stress in the mechanically stable copolyimide.

For these copolyimides, residual stress increased in the range of −5 to 50 MPa, whereas stress relaxation induced

Table 4
Thermal expansion properties and glass transition temperature of PMDA/ 6FDA-PDA copolyimide by thermal imidization at 400°C for 1 h

Molar ratio PMDA/6FDA	Elongation (%)	T_g (°C) by DMTA	Thickness (μm)
0/100	3.12	375	10.3
30/70	2.10	430	11.3
50/50	1.07	450	11.0
70/30	1.05	> 460	11.2
90/10	0.91	–	10.9
100/0	0.81	–	10.7

by water uptake decreased in the range of 20.5–4.5 MPa with increasing 6FDA compositions, respectively. The stress relaxation results due to water uptake indicated that PMDA-PDA absorbs more water than 6FDA-PDA, and their compolyimides showed stress relaxation intermediate between those of both components. This indicated that chain mobility during thermal process is also important to the degree of stress relaxation due to water uptake. Overall, the major factor in determining the magnitude of the stress behavior induced by both the thermal mismatch and water diffusion in films should be the morphological factor such as in-plane orientation, crystallinity, molecular packing order and microvoids. The degree of in-plane chain orientation is directly correlated to the residual stress and stress relaxation coefficient (*S*) in the film, which is an in-plane characteristic. However, the stress relaxation caused by the water uptake is significantly influenced by packing order due to restricted chain mobility or chain organization, which might occur during thermal imidization. Their morphological structures were examined by WAXD and prism coupler, and for thermal properties using DMTA and TMA. In conclusion, both the 90/10 (=PMDA/6FDA in molar ratio) and 30/70 composition of the PMDA/6FDA-PDA copolyimide films, which had the low level stress showed the possibility in potential application as encapsulant, stress-relief buffer, and interlayer dielectrics. However, the degree of stress relaxation induced by water uptake still remained high because the imidized copolyimide chains had higher T_g than the final imidization temperature (400°C) during thermal imidization. Under this circumstance, microvoids generated in thermal imidization process may not be healed completely.

Acknowledgements

This work was supported by a grant Brain Korea 21 Project.

References

[1] Mittal KL. Polyimides: synthesis, characterization and application. New York: Plenum Press, 1984.
[2] Wilson D, Stenzenberger HD, Hergenrother PM. Polyimides. New York: Chapman & Hall, 1990.
[3] Pryde CA. J Polym Sci Part A: Polym Chem 1989;27:711.
[4] Brekner J, Feger C. J Polym Sci Part A: Polym Chem 1987;25:2005.
[5] Han H, Gryte CC, Ree M. Polymer 1995;36:1663.
[6] Han H, Chung H, Gryte CC, Shin TJ, Ree M. Polymer 1999;40:2681.
[7] Chang YL, Jou JH. J Polym Sci Part B: Polym Phys 1994;32:2143.
[8] Denton DD, Day DR, Priore DF, Senturia SD, Anolick ES, Scheider D. J Electron Mater 1985;14:119.
[9] Ree M, Chu CW, Goldberg MJ. J Appl Phys 1994;75:1410.
[10] Elsner G. J Appl Polym Sci 1987;34:815.
[11] Sackinger ST, Farris RJ. Polym Mater Sci Engng 1987;57:356.
[12] Numata S, Fujisaki K, Kinjo N. Polymer 1987;28:2282.
[13] Sykes CF, Clair AKST. J Appl Polym Sci 1986;32:2735.
[14] Hedrick JL, Brown HR, Volksen W, Sanchez M, Plummer CJG, Hilborn JG. Polymer 1997;38:605.
[15] Yang CP, Hsiao SH. J Appl Polym Sci 1986;31:979.
[16] Chung H, Joe Y, Han H. J Appl Polym Sci 1999;74:3287.
[17] Chung H, Joe Y, Han H. Polym J 1999;31:700.
[18] Chung H, Joe Y, Han H. Polym J 2000;32:215.
[19] Chung H, Lee J, Jang W, Shul Y, Han H. J Polym Sci Part B: Polym Phys 2000;38:2879.
[20] Ree M, Shin TJ, Park YH, Kim SI, Woo SH, Cho CK, Park CE. J Polym Sci Part B: Polym Phys. 1998;36:1261.
[21] Costello LM, Koros WJ. J Polym Sci Part B: Polym Phys 1995;33:135.
[22] Lokhandwala KA, Nadakatti SM, Stern SA. J Polym Sci Part B: Polym Phys 1995;33:965.
[23] Becker KH, Schmidt HW. Macromolecules 1992;25:6784.
[24] Ree M, Nunes TL, Chen KR. J Polym Sci Part B: Polym Phys 1995;33:453.
[25] Chung H, Lee C, Han H. Polymer 2001;42:319.
[26] Jou JH, Huang R, Huang PT, Shen WP. J Appl Polym Sci 1991;43:857.
[27] Timoshenko SP. J Opt Soc Am 1926;11:223.
[28] Wortman JJ, Evans RA. J Appl Phys 1965;36:136.
[29] Crank J. The mathematics of diffusion. Oxford, UK: Clarendon, 1964.
[30] Crank J, Park GS. Diffusion in polymer. London: Academic Press, 1968.
[31] Neogi P. Diffusion in polymer. New York: Marcel Dekker, 1996.
[32] Cullity BD. Elements of X-ray diffraction. 2nd ed. Reading, MA: Addison-Wesley, 1978.
[33] Takahashi N, Yoon DY, Parrish W. Macromolecules 1994;17:2583.
[34] Poittiger MT, Coburn JC, Edman JR. J Polym Sci Part B: Polym Phys 1994;32:826.
[35] Cha CY, Samuels RJ. J Polym Sci Part B: Polym Phys 1995;38:259.
[36] Hardaker SS, Moghazy S, Cha CY, Samuels RJ. J Polym Sci Part B: Polym Phys 1993;31:1951.
[37] Moylan CR, Best ME, Ree M. J Polym Sci Part B: Polym Phys 1991;29:87.
[38] Burrel. Polymer handbook. 2nd ed. New York: Wiley-Interscience, 1975.
[39] Ree M, Han H, Gryte CC. J Polym Sci Part B: Polym Phys 1995;33:505.